Dalton Transactions

Accepted Manuscript

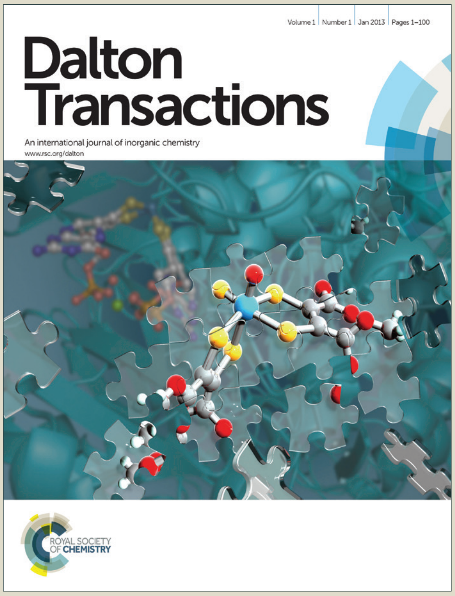

ROYAL SOCIETY OF CHEMISTRY

www.rsc.org/dalton

Detecting gas molecules via atomic magnetization

Heechae Choi[1,2], Minho Lee[2], Seungchul Kim[1*], Kwang-Ryeol Lee[1], and Yong-Chae Chung[2*]

AUTHOR ADDRESS

[1]Center for Computational Science, Korea Institute of Science and Technology, Hwarangro 14 Gil 5, Seoul 136-791, Korea

[2]Department of Materials Science and Engineering, Hanyang University, 17 Haengdangdong, Seoul 133-791, Korea

KEYWORDS: Magnetic property, Gas sensing, *Ab initio* calculations, Density functional theory, Graphene

ABSTRACT: Adsorptions of gas molecules were found to alter the directions and magnitudes of magnetic moments of transition metal (Co, Fe) atoms adsorbed on graphene. Using first-principles calculations, we demonstrated that magnetism of surface atoms can be used to identify the kind of the existing gas molecules via spin-reorientation and/or demagnetizations as the results of the reconfigurations of 3*d* electron energy levels of Co and Fe. We suggest as the first time that magnetic properties of transition metal embedded nanostructures can be used in highly selective gas sensing applications.

Email: yongchae@hanyang.ac.kr, sckim@kist.re.kr

1. Introduction

Conventional gas sensors using electrical conductivity distinguish certain kinds of existing gas species by the changes electric current. In general, the electricity based gas sensors have poor selectivity, causing them to respond to multiple analytes, which is called cross-sensing.[1-4] Especially, toxic gas sensors should be able to exclusively respond to target gas molecules neglecting atmospheric gases, such as H_2O, O_2, and $N_{2.}$[1-2] Most of the improvements in the selectivity of toxic gas sensors have been achieved by modifying the device architectures[5] or using new kinds of nanomaterials such as carbon nanotubes and semiconductor nanowires.[2-4] Employing a new kind of property instead of continuously using electric current, in spite of very few numbers of reports being published so far, is said to be the most challenging and innovative way to improve the selectivity of chemical sensing devices. Even if the selectivity on a property is poor when used in gas mixtures, the cross-sensitivity does not exist on all properties, and thus the overall sensing result can distinguish target gas species with far better accuracy. In addition, finding a new kind of property to use in gas sensors can broaden the candidate materials and give more possibility of cost-effective designs of devices.

Spin degree of freedom in devices has provided higher bits of information than the binary on/off signals by electric currents.[8-11] Here, we try to use electron orbital configurations, which have higher degree of freedom than electric current, in the gas molecule detections. The resultant *signal* is the magnetic properties of transition metal (TM) atoms which are capable of forming chemical bonds with multiple gas species. Our first-principles calculations show that the orientations and magnitudes of magnetizations of transition metal atoms on graphene are changed by the adsorptions of CO, NO, and NO_2 gas molecules by the reconfigurations of 3*d* electron energy levels. The configurations of 3*d* electron levels make *signals* distinguishable them from atmospheric gas species (H_2O, O_2, N_2). The single transition metal atoms (Co, Fe) adsorbed on graphene were chosen for magnetic gas detections in this study, due to the following reasons: i) large surface/volume ratio of graphene sheet[11, 12] , which is a great advantage for a gas sensing material, ii) stronger adsorptions of toxic gas molecules of our interest (CO, NO, NO_2) on metal atoms than on graphene surface[13-17], and iii) tunable electron configurations of Co and Fe when being adsorbed on graphene surface so that π-bonds become easier in upward direction with strong π-accepting CO and NO molecules.[1-2, 6]

Due to the tiny magnetic anisotropy energies of the prototype of nanomagnetism, magnetic adatoms on graphene, the temperature of operation is less than few tens of K. However, our first exploration to use magnetism in gas sensing is expected to allow us wider choice of gas sensing materials out of pre-existing nanomaterials.

2. Calculation method

Density functional theory (DFT) calculations in this study were performed using generalized gradient approximation (GGA) with the projector augmented wave (PAW) pseudopotential method.[25] The PAW method allows to use moderate cut-off energies in the construction of the plane wave basis. All calculations were performed with the Vienna ab initio simulation package (VASP)[26] using a plane wave cut-off energies of 500.0 eV (29.4 Ry). In 4 × 4 graphene supercell, the Brillouin-zone integrations were performed using the 4 × 4 × 1 and 14 × 14 × 1 Monkhorst-Pack scheme for structure relaxations and electronic structure calculations, respectively.[27] Positions of atoms were relaxed using the conjugate gradient method until all Hellmann-Feynman forces become smaller than 0.01 eV/Å. The effective range of the cutoff energy and the validity of the mesh density used in our calculations were determined by a convergence test using the theoretically estimated lattice constants of pristine graphene, 2.464 Å. The supercell of the single layer graphene in this study consists of 32 carbon atoms and the most stable adsorption site of Co and Fe atoms was both on the center of a hexagonal carbon ring (Figure. 1). The constructed supercells were periodically repeated with a 15 Å vacuum spacer lying along the vertical direction. For the noncollinear magnetism calculations, the spin-orbit coupling (SOC) term was explicitly included. Since SOC is a short-range interaction, a cell with 32 carbon atoms was found to be large enough for a study on spin switching of single TM atoms from our test calculations, which showed differences in magnetic anisotropic energy (MAE) and magnetic moments of Co and Fe less than 10 % in magnitudes from those on the cells with 16 and 24 carbon atoms.

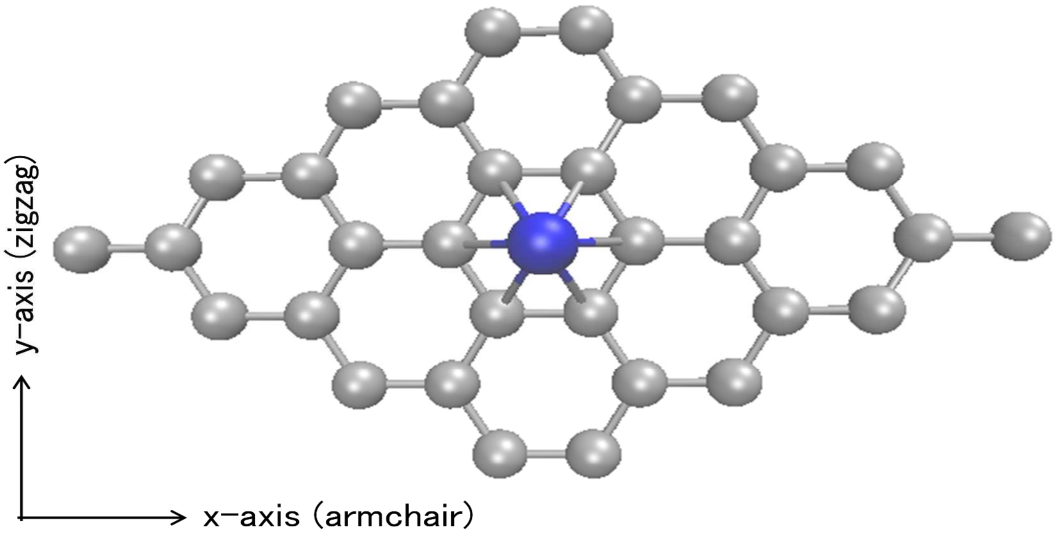

Figure 1. Topview of the TM (Co, Fe) adatoms on graphene. The blue and grey spheres are a TM adatom and graphene C atoms.

3. Results and Discussions

The stable atomic structures of gas-adsorbed TM@G were obtained by choosing the lowest energy configuration among several (three to six) trial structures of each gas molecule on each TM@G: placing two opposite directions of vertical alignments, parallel to graphene plane, or in-plane rotation about to the hexagonal ring of graphene. The optimized atomic structures of gas-adsorbed TM@G systems are presented in Figure 2. The atomic structures of gas-adsorbed Co@G and Fe@G were similar. The NO_2 molecule is adsorbed on TM@G with two oxygen atoms bonded to TM atoms, and O-N-O aligns along the AC direction of graphene lattice. N_2 and O_2 molecules prefer in-plane alignments along the zigzag (ZZ) and armchair (AC)-directions of graphene lattice, respectively. The energy differences between the ZZ- and AC- alignments of N_2 and O_2 molecules were below 0.05 eV. CO and NO prefer bindings of C and N atoms to TM adatoms in vertical directions with significant amount of energy difference from the opposite direction: 0.12eV for CO on Co@G; 1.86 eV for NO on Co@G; 0.14eV for CO on Fe@G; 1.73 eV NO on Fe@G. The H_2O molecule prefers O-TM bindings on graphene while O-H arms align along AC direction. N atom in NH_3 molecule bonds to TM, and N-H bonds align along ZZ direction. TM adsorption little modifies graphene structure. The maximum elevation of carbon atoms (Δz_{max}) is just 0.11 Å, as it is down in Figure 2, and it is much smaller than 0.1 Å for most cases.

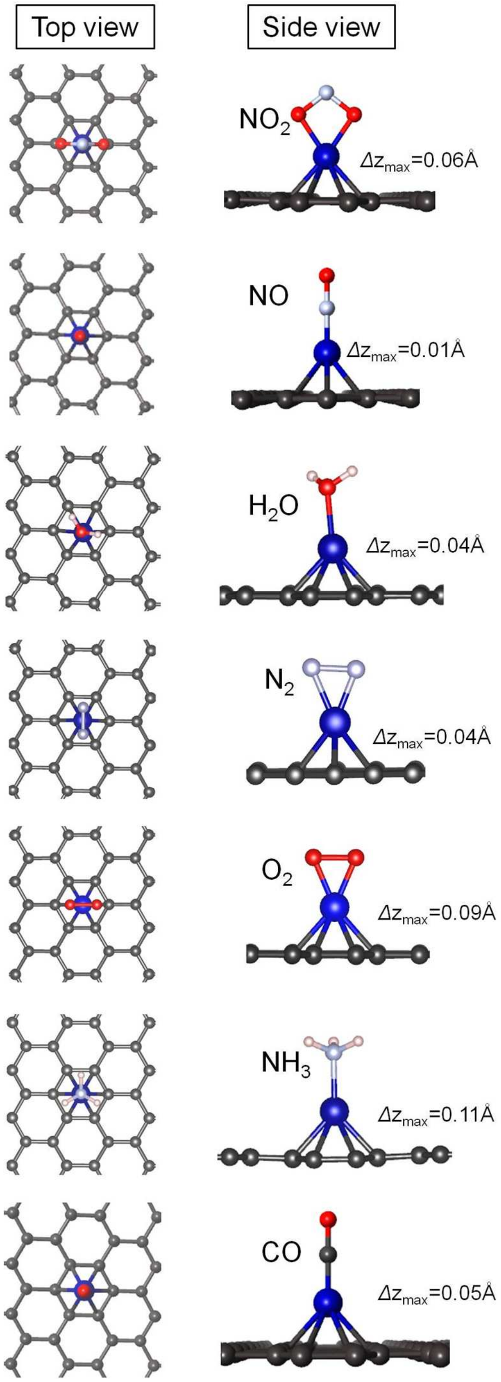

Figure 2. Top and side views of gas-adsorbed TM@G systems obtained via geometry optimization processes. The dark grey, blue, red, pink, and ice blue sphene indicate the C, TM, O, H, and N atoms, respectively. ΔZ_{max} is the maximum elevation of carbon atoms in graphene from the graphene plan.

We investigated the magnetic properties and electron configurations of Co and Fe atoms on graphene (Co@G and Fe@G), using the DFT calculations. As summarized in Table I, the electron configurations of Co and Fe were changed to $3d^9$ and $3d^8$, as the electrons in $4s$-orbitals of Co and Fe are transferred to the $3d$ orbitals as being adsorbed on the hollow site of pristine graphene sheet, the most stable adsorption site. The magnetic moment of Co@G (1.0 μ_B) is from the unpaired electron in the Co $3d_{yz}$ and $3d_{zx}$ orbitals, whose minority-spin states are partially populated above the Fermi level (Figure 4). Similarly, Fe@G has minority-spin states in $3d_{yz}$ and $3d_{zx}$ orbitals populate clearly above the Fermi level, which leads to 2.1 μ_B of magnetic moment of Fe adatom. The calculated differential charge isosurface shows that the changed electronic configurations are not originated from the charge transfer between graphene sheet and the TM adatoms but from the reconfigurations of electrons of TM adatoms ($4s$ to $3d$ orbtial) (See Supplement 1). The magnetic easy axes of Co@G and Fe@G are in the perpendicular and zigzag (ZZ) directions, respectively due to the main contributions of spin-orbit coupling (SOC) term to the magnetic anisotropy energy (MAE). The calculated perpendicular magnetic anisotropy energy (PMAE), the energy difference between the systems with perpendicular and in-plane magnetizations, of Co@G and Fe@G were 0.69 and -0.90 meV/atom, respectively. The total energy difference of a system with in-plane and perpendicular magnetization, PMAE, was calculated using the equation,

$$\mathrm{PMAE} = E_{\parallel} - E_{\perp},$$

where $E_{\parallel}$ and $E_{\perp}$ are the system total energies with in-plane and perpendicular directions of magnetic moments, respectively. It may be difficult to distinguish the atomic spin directions on graphene between armchair and zigzag directions using, for example, spin-polarized scanning tunnel microscopy (SP-STM)[25-26], due to the small in-plane angle difference, 30° in the honeycomb structure. Instead, we assumed that the switching of spin directions of the TM@G from perpendicular to in-plane directions or vice versa is more suitable signal that can be more easily measurable.

System	Electron configuration	Magnetic moment (μ_B)	m_L (∥)	m_L (⊥)	PMAE
Co@G	$3d^9$	1.0	0.12	1.02	0.69
Fe@G	$3d^8$	2.1	0.13	0.05	-0.90

Table I Electron configurations, magnitude of spin magnetic moments (m_s), in-plane (m_L (∥)) and perpendicular direction (m_L (⊥)) components of magnetic moments, and perpendicular magnetic anisotropic energy (PMAE).

The high adsorption energy of a gas molecule on a gas sensor is an important feature for high-speed detection.[27,28] We obtained the adsorption energies of gas molecules on the TM adatoms, in order to investigate the possibility of TM@G system to be used in high-speed sensing compared to the conventional graphene or graphene nanoribbon (GNR) sensor systems.[17, 27, 28] All of the gas species considered in this study binds to TM adatoms on graphene, with much higher adsorption energies than on graphene surface and even than functionalized GNR edges. These preferences of gas molecules to adsorb on TM atoms are similar to those in noble metal embedded graphene systems, as summarized in Table II. Since the gas coverage rate is proportional to the adsorption energy, TM@G systems have a capability to uptake gas molecules more quickly than graphene gas sensors, which detect gas molecules via electricity.

	O_2	**H_2O**	**NO**	**NO_2**	**CO**	**NH_3**
Pristine graphene [Ref.17]	< 0.1	-	0.30	0.48	0.12	-0.02
B-doped graphene [Ref. 27]	0.01	0.04	1.07	0.33	0.02	0.02
Functionalized GNR [Ref.28]	1.88	-	2.29	2.70	1.34	0.18
Co/grephene (this work)	3.63	0.80	4.41	3.15	2.46	0.98
Fe/graphene (this work)	3.75	0.77	3.93	3.23	2.16	1.55

Table II. Adsorption energies of gas molecules on graphene-based materials.

		O_2	N_2	CO	NO_2	NO	H_2O	NH_3
Co@G	PMAE (meV/atom)	-0.36	-1.11	-0.29	-	-	0.64	1.05
	m_s	0.8	1.0	1.0	0	0	1.0	1.1
	Δm_L	0.06	0.12	0.05	0	0	-0.08	-0.10
Fe@G	PMAE (meV/atom)	-0.20	0.25	0.38	-0.36	0.60	-0.14	-0.26
	m_s	1.5	2.1	2.1	1.0	1.3	1.4	2.2
	Δm_L	0.04	-0.02	-0.05	0.02	-0.05	0.02	0.03

Table III. Magnetic properties of Co@G and Fe@G with gas molecule adsorptions.

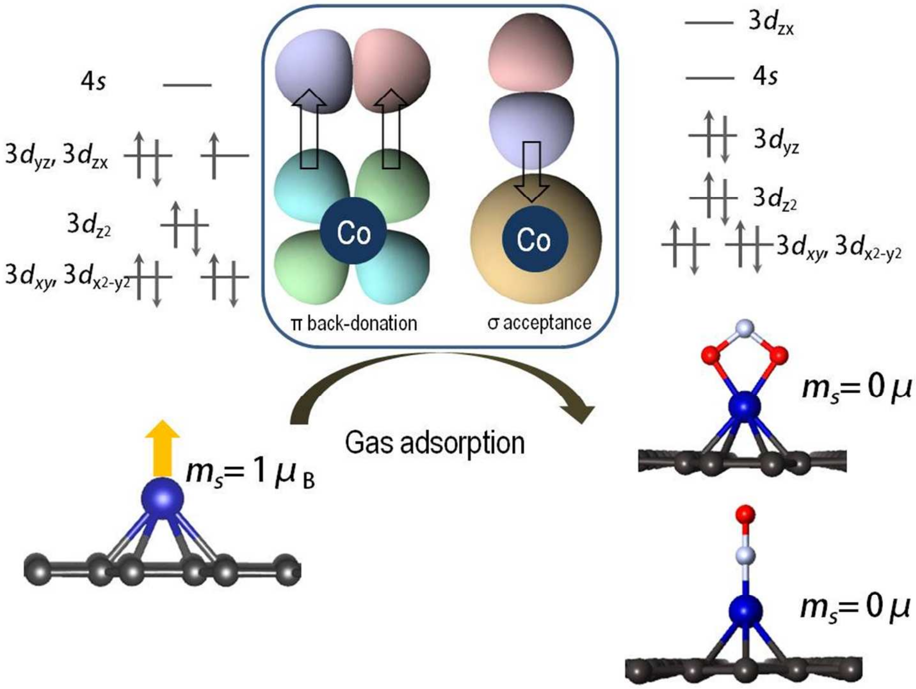

Figure 3. Schemes of charge transfers between Co@G and NO or NO_2 molecule via π- and σ-bonding (Top) and the electron configurations (Middle) and atomic structures (Bottom) of Co@G and NO- and NO_2- adsorbed Co@G.

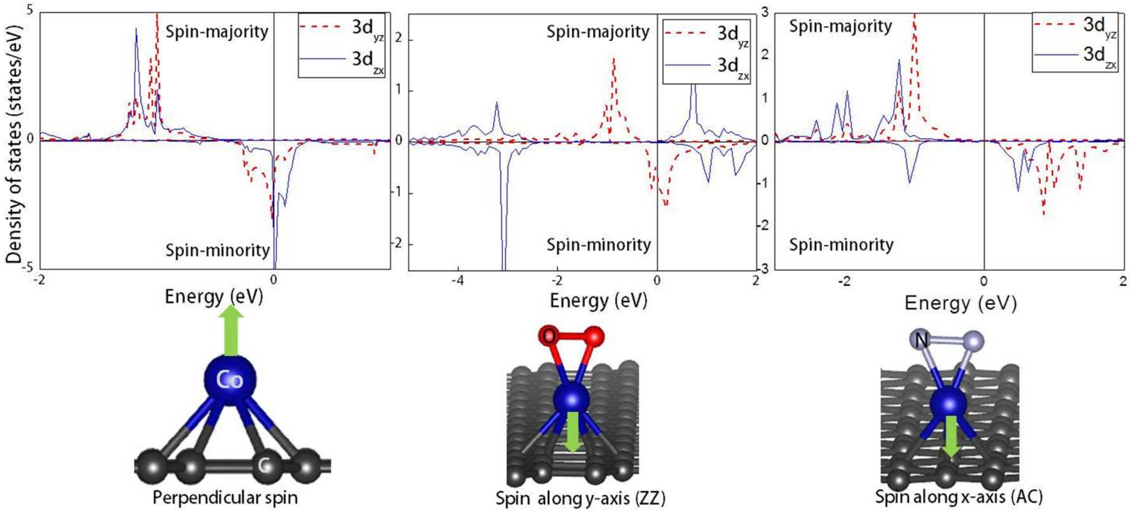

Figure 4. The atomic structures of O_2 and N_2 on Co@G and DOS of Co@G before and after the adsorptions of O_2 and N_2.

As the next step, we investigated how the electron configurations and magnetizations of the TM@G are changed by the adsorptions of the gas molecules. The calculated PMAE, spin magnetic moments, and the adsorption energies of gas molecules, which can be detected using the magnetism of TM@G are summarized in Table III. The adsorptions of NO and NO_2 on Co@G turns the Co adatom nonmagnetic ($m_s = 0$) by accepting electrons from Co via π- bonds (Figure 3). As the results, the unpaired electron spin in the highest occupied atomic orbital ($3d_{zx}$ orbital) is transferred to the adsorbed gas molecules. On the other hand, the adsorptions of O_2 and N_2 molecules on Co@G switched the spin direction of Co from perpendicular to in-plane direction as the $3d_{zx}$ and $3d_{yz}$ electrons in Co@G are transferred to $2p_z$ orbital of adsorbed O_2 and N_2 molecules (Figure 4). When graphene accommodates chemisorptions of gas molecules, such as oxygen or hydrogen, the structures are deformed and the sizeable magnetic moments (upto $1\mu_B$ per atom) are induced depending on the degree of bending or fluctuations.[29, 30] However, such the atmospheric gas chemisorptions on graphene are hindered by large kinetic energy barriers. Also, defect free graphene is chemically inert, so most of gas molecules do not react with graphene spontaneously in ambient condition. Therefore, we can expect that the magnetic signals from TM@G are not confused by the chemisorptions-induced magnetization of graphene sheet.

As it is indicated by the positive PMAE values of Fe@G, the in-plane magnetization of Fe@G is switched to perpendicular direction when CO and NO are adsorbed.

Figure 5 shows the spin switching in Fe@G by the adsorptions of CO and NO that minority spin states of $3d_{zx}$ and $3d_{yz}$ shift downward below the Fermi level and minority spin states of $3d_{z2}$ shift above the Fermi level. The Fe@G system, however, does not show the changes in magnetization with O_2 adsorption. The adsorptions of NH_3, H_2O, and CO_2 molecules on Co@G and Fe@G do not frustrate or rotate the spin moment of Co@G and Fe@G. In other words, three of the target gas molecules (CO, NO, NO_2) can be selectively detected even in the existence of atmospheric gas environments (H_2O, O_2, N_2).

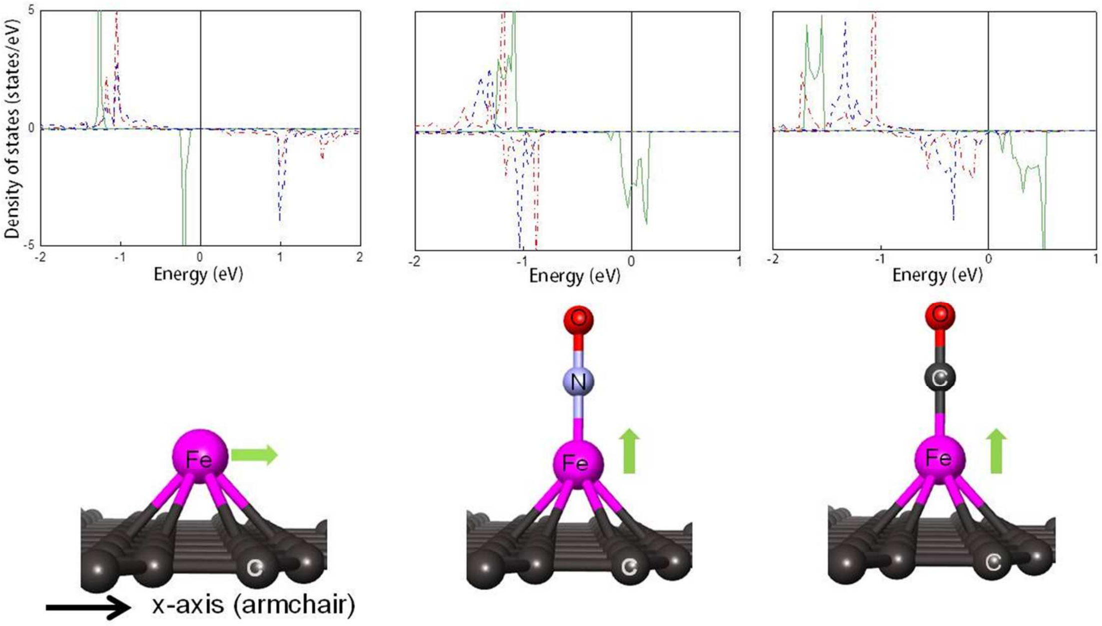

Figure 5. The atomic structures and spin directions of Fe@G, and CO- and NO- adsorbed Fe@G (bottom) and the corresponding electron density of states of Fe (top).

The methods to detect of NO, NO_2, CO, O_2 molecules using the combined signals of Co@G and Fe@G magnetizations are summarized in Table III. With signals of $m_s = 0$ in Co@G and the spin reorientations of Fe@G to perpendicular direction, NO and NO_2, can be selectively identified. Only CO aligns the spin directions of both Co@G and Fe@G in perpendicular directions, which can be interpreted as the identical signal for CO molecule. Since the adsorption of O_2 or N_2 on Co@G and Fe@G both aligns the spin directions to in-plane, the existences of O_2 and N_2 also can be known.

Co@G	Fe@G	Existing gas
$m_s = 0$	Perpendicular	NO
$m_s = 0$	In-plane	NO_2
Perpendicular	Perpendicular	CO
In-plane	In-plane	O_2 or N_2

Table III. Detections of NO, NO_2, CO, and O_2 using the changes in the magnitude and directions of Co@G and Fe@G.

4. Conclusion

Using the first-principles calculations, we investigated how the magnetic properties of Co and Fe adatoms on graphene are changed by adsorptions of gas molecules (O_2, H_2O, NO, NO_2, CO, N_2, NH_3). The measurable changes in the electronic spins of Co@G and Fe@G were found to give distinguishable signals for CO, NO, and NO_2 molecules by the chemisorptions and resulting reconfigurations of 3*d*- and 4*s*- orbital electrons of Co@G and Fe@G. Here, we suggest that gas detection using materials' magnetic properties can make breakthroughs for highly selective and low-power-consuming gas sensor systems due to the higher degree of freedom of 3*d*-orbital electron configuration We expect that similar advanced works with other nanomaterials such as magnetic semiconductors, oxides[29] or defective carbon structures[30] can overcome such barriers.

ACKNOWLOGEMENTS

H. Choi was supported by internal project of Institute for Multidisciplinary Convergence of

Matter (IMCM) of Korea Institute of Science and Technology (KIST), Exploratory & Creative Research(Grant No.2E23392). S. Kim and K.-R. Lee were supported by the Converging Research Center Program through the Ministry of Science, ICT and Future Planning, Korea (Grant No. 2013K000176). M. Lee and Y.-C. Chung were supported by Basic Science Research Program of National Research Foundation (NRF) of Korea (NRF-2014R1A1A2A10064432).

REFERENCES

1 Boyle, J. F. & Jones, K. A. The effects of CO, water vapor and surface temperature on the conductivity of a SnO_2 gas sensor. *J. Elect. Mater.* **6**, 717-733 (1977).

2 Wang, X. *et al.* Batteryless chemical detection with semiconductor nanowire. *Adv. Mater.* **23**, 117-121 (2011).

3 Zhang, T., Mubeen, S., Myung, N. V. & Deshusses, M. A. Recent progress in carbon nanotube-based gas sensor. *Nanotechnology* **19**, 332001-332014 (2008).

4 Schedin, F., *et al*. Detection of individual gas molecules adsorbed on graphene. *Nat. Mater.* **6**, 652-655 (2007).

5 Alain, G., Shim, C. H., Philippe, M. & François L. Chemoresistor type gas sensor having a multi-storey architecture. *European Patent. 2 533 037 A1* Dec 12 2012.

6 Baibich, M. N., Broto, J. M., Fert, A., Nguyen Van Dau, F., & Petroff, F. Giant magnetoresistance of (001)Fe/(001)Cr magnetic superlattices. *Phys. Rev. Lett.* **61**, 2472-2475 (1988).

7 Wu, S. M., *et al.* Reversible electric control of exchange bias in a multiferroic field-effect device. *Nat. Mater.* **9**, 756-761 (2010).

8 Wolf, S. A. *et al*. Spintronics: A spin-based electronics vision for the future. *Science* **294**, 1488-1495 (2001).

9 Gambardella, P. *et al.* giant magnetic anisotropy of single cobalt atoms and nanoparticles. *Science* **300**, 1130-1133 (2003).

10 Meier, F., Zhou, L., Wiebe, J. & Wiesendanger, R. Revealing magnetic interactions from single-atom magnetization curve. *Science* **320**, 82-86 (2008).

11 Balashov, T. *et al*. Magnetic anisotropy and magnetization dynamics of

indivisual atoms and cluster of Fe and Co on Pt (111). *Phys. Rev. Lett.* **102**, 257203-257206 (2009).

13 Ratinac, K. R., Yang, W., Ringer, S. P. & Braet, F. Toward ubiquitous environmental gas sensors-capitalizing on the promise of graphene. *Environ Sci. Technol.* **44**, 1167-1176 (2010).

14 Zhang, Y. H., *et al*. Improving gas sensing properties of graphene by introducing dopants and defects: a first-principles study. *Nanotechnology* **20**, 185504-185512 (2009).

15 Ji, Q., *et al*. Layer-by-layer films of graphene and ionic liquids for highly selective gas sensing. *Angew. Chem.* **122**, 9931-9933 (2010).

16 Lu, Y., Goldsmith, B. R., Kybert, N. J. & Johnson, A. T. C. DNA-decorated graphene chemical sensors, *Appl. Phys. Lett.* **97**, 083107-083109 (2010).

17 Zhou. M., Lu, Y. H., Cai, Y. Q., Zhang, C. & Feng, Y. P. Adsorption of gas molecules on transition metal embedded graphene: a search for high-performance graphene-based catalysts and gas sensors. *Nanotechnology* **22**, 385502-385509 (2011).

18 Perdew, J. P. *et al.* Atoms, molecules, solids, and surfaces: Applications of the generalized gradient approximation for exchange and correlation. *Phys. Rev. B* **46**, 6671 (1992).

19 Perdew, J. P., Burke, K. & Ernzerhof, M. Generalized gradient approximation made simple. *Phys. Rev. Lett.* **77**, 3865-3868 (1996).

20 Kresse, G. & Joubert, D. From ultrasoft pseudopotentials to the projector augmented-wave method. *Phys. Rev. B* **59**, 1758-1775 (1999).

21 Kresse, G. & Furthmuller, J. Efficient iterative schemes for ab initio total-

energy calculations using a plane-wave basis set. *Phys. Rev. B* **54**, 11169-11186 (1996).

22 Monkhorst, H. J. & Pack, J. D. Special points for Brillouin-zone integrations. *Phys. Rev. B* **13**, 5188 (1976).

23 Valencia H., Gil. A. & Frapper G. Trends in the adsorption of 3d transition metal atoms onto graphene and nanotube surfaces: a DFT study and molecular orbital analysis. *J. Phy. Chem. C* **114**, 14141-14153 (2010).

24 Tang, S. & Cao, Z. Adsorption of nitrogen oxide on graphene and graphene oxides: insights from density functional calculations. *J. Chem. Phys.* **134**, 044710-444724 (2011).

25 Gambardella, P., *et al.* Supramolecular control of the magnetic anisotropy in two-dimensional high-spin Fe arrays at a metal interface. *Nat. Mater.* **8**, 189-193 (2009)

26 Hirjinbehedin, C. F. *et al.* Large magnetic anisotropy of a single atomic spin embedded in a surface molecular network. *Science* **317**, 1199-1203 (2007).

27 J. Dai, J. Yuan, and P. Giannozzi, Gas adsorption on graphene doped with B, N, Al, and S:A theoretical study, *Appl. Phys. Lett.* **95**, 232105-232107 (2009).

28 B. Huang, Z. Li, Z. Liu, G. Zhou, S. Hao, J. Wu, B.-L. Gu, and W. Duan, Adsorption of Gas Molecules on Graphene Nanoribbons and Its Implication for Nanoscale Molecule Sensor, *J. Phys. Chem. C* **112**, 13442-13446 (2008).

29 Yazyev, O. V. & Helm, L. Defect-induced magnetism in graphene. Phys. Rev. B **75**, 125408 (2007).

30 Punnoose, A., Reddy, K. M., Hays, J., Thunber, A., & Engelhard, M. H., Magnetic gas sensing using a dilute magnetic semiconductor. *Appl. Phys. Lett.* **89**, 112509 (2006).

31 Minkyung. Choi, Jangyup. Son, Heechae Choi, Hyun-Joon Shin, Sangho Lee, Sanghoon Kim, Soogil Lee, S. Kim, Kwang-Ryeol Lee, Sang Jin Kim, Byung Hee Hong, Jongill Hong, and In-Sang Yang, *J. Raman Spectrosc.* **45**, 168-172 (2014).

32 Ž. Šljivančanin, R. Balog, L. Hornekær, Magnetism in graphene induced by hydrogen adsorbates, Chem. Phys. Lett. **541**, 70-74 (2012).

33 Schiros, T. et al., Conneting Dopant Bond Type with Electronic Structure in N-doped Graphene, *Nano Lett.* **12**, 4025-4031 (2012).

34 Gao, H. et al., A simple method to synthesize continuous large area nitrogen-doped graphene, *Carbon* **50**, 4476-4482 (2012).